The initiation and propagation of adiabatic shear bands (ASBs) in functionally graded materials (FGMs) deformed at high strain rates in plane strain tension have been studied by the finite element (FE) method. An ASB is a narrow region, usually a few microns wide, of intense plastic deformation that forms after softening of the material due to heating and damage evolution has overcome its hardening due to strain- and strain-rate effects. ASBs usually precede ductile fracture. The volume fraction of each phase varies continuously in a cross-section. Each constituent and the composite are modeled as isotropic, microporous, strain- and strain-rate hardening, and thermally softening materials with effective properties of the composite derived either by the rule of mixtures or from studying deformations of a representative volume element. Each phase and the homogenized composite obey the Johnson-Cook thermoviscoplastic relation, Gurson's type flow potential, the associated flow rule, and a hyperbolic heat equation. Thermoelastic material parameters of the composite are assumed to degrade with the evolution of the porosity which is taken to represent the damage. No initial defect is introduced.

Results have been computed for tungsten (W) particles interspread in a NiFe matrix with the volume fraction of NiFe given by one of the following two expressions:

Type I

$$v_{f,NiFe} = \begin{cases} c\dfrac{r}{H}, & r < H \\ c, & r \geq H \end{cases}$$

Type II

$$v_{f,NiFe} = \begin{cases} c\left(1 - \dfrac{r}{H}\right), & r < H \\ 0, & r \geq H \end{cases}$$

Here r is the radial distance from the specimen centroid, and 2H equals the length of a side of the square cross-section. In both type-I and type-II FGMs, material properties in the region r > H are constants. In type-I FGMs, the volume fraction of NiFe varies from zero at the specimen centroid to c at r = H, and in type-II FGMs, it varies from c at the specimen centroid to zero at r = H.

The developed code has been verified by comparing computed results with those available in the literature. Results presented below are with a uniform FE mesh of 1600 4-node quadrilateral elements. Results computed with a finer mesh of 6400 elements changed the ASB initiation time by less than 1%. For reference and to delineate the effect of the initial porosity distribution, Table 1 lists the ASB initiation times for five materials. It is clear that an ASB initiates considerably sooner in initially porous materials than in those with zero initial porosity. Also, tungsten is most susceptible to shear banding and Armco iron the least.

Table 1. Axial strain at ASB initiation in five homogeneous materials

| Material | Axial strain at ASB initiation in plane strain tension | |
|---|---|---|
| | nonuniform initial porosity | zero initial porosity |
| Tungsten (W) | 0.137 | 0.386 |
| 4340 steel | 0.315 | 0.615 |
| Nickel iron | -- | 0.944 |
| OFHC copper | 0.391 | 1.045 |
| Armco iron | 0.433 | 1.095 |

Numerical experiments on type-I and type-II FGMs yielded interesting results summarized in Table 2. In the first subset of tests on type-I FGMs, the maximum volume fraction,c, of NiFe was varied from 0.1 to 0.5. In each case, an ASB initiated at the specimen centroid and propagated along a line inclined at 45º to the horizontal axis in the present configuration. However, the axial strain at the instant of ASB initiation decreased monotonically with an increase in the maximum volume fraction of NiFe at the centroid. Contours of the effective plastic strain in a type-I FGM are depicted in Fig. 1. The effective plastic strain within the ASB exceeds 1 with a peak value of 1.4 at some points. For type-II FGMs with the maximum volume fraction of NiFe at the centroid, an ASB initiated from a point on the top surface and propagated inwards along the two directions of the maximum shear stress. As shown in Fig.2, there are several narrow regions of intense plastic deformation. The point where an ASB initiated on the top surface varied with the compositional profile. Results for numerical experiments on other type-I FGMs containing different matrix material are also summarized in Table 2. Of the FGMs studied, the type-I with NiFe matrix delays most the onset of an ASB and that with copper matrix the least. Composites comprised of tungsten in the region

r <5 and NiFe elsewhere or vice-a-versa were also analyzed. In these an ASB initiated from different points on the top surface and propagated inwards in two directions.

The numerical tests reveal that the addition to pure tungsten of a material less susceptible to shear banding than tungsten delays the initiation of an ASB in the composite. The analysis can be used to optimize the compositional profile to either delay or to enhance the onset of an ASB.

Table 2. Axial strain and the point of initiation of ASBs in FGMs

| Specimen type and constituents | Max. $v_f$ of NiFe | Axial strain at ASB initiation | Point of ASB initiation (ref. config) | |
|---|---|---|---|---|
| | | | X | Y |
| W/NiFe Type I | 0.1 | 0.371 | 0.000 | 0.000 |
| | 0.2 | 0.339 | 0.000 | 0.000 |
| | 0.3 | 0.327 | 0.000 | 0.000 |
| | 0.4 | 0.325 | 0.000 | 0.000 |
| | 0.5 | 0.331 | 0.000 | 0.000 |
| W/NiFe Type II | 0.1 | 0.340 | 1.125 | 5.000 |
| | 0.2 | 0.314 | 1.250 | 5.000 |
| | 0.3 | 0.304 | 1.375 | 5.000 |
| | 0.4 | 0.298 | 4.750 | 2.875 |
| | 0.5 | 0.292 | 4.875 | 2.875 |
| W/4340 Type I | 0.3 | 0.364 | 1.125 | 5.000 |
| W/NiFe Type I | 0.3 | 0.327 | 0.000 | 0.000 |
| W/Cu Type I | 0.3 | 0.218 | 0.625 | 5.000 |
| W/Fe Type I | 0.3 | 0.268 | 1.000 | 5.000 |

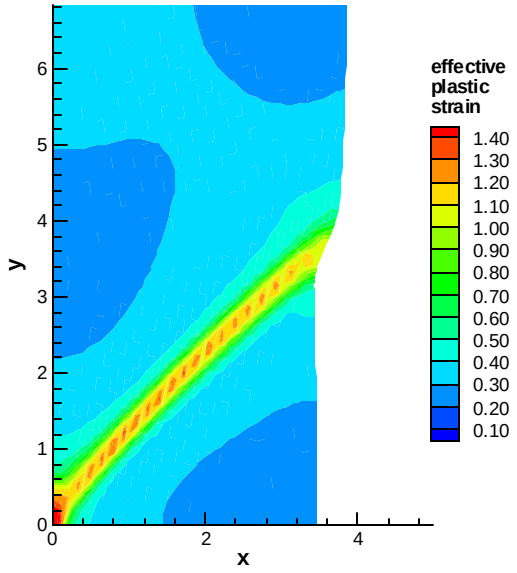


Figure 1. Contours of effective plastic strain for a type-I W/NiFe FGM with c = 0.3 at an axial strain of 0.40.

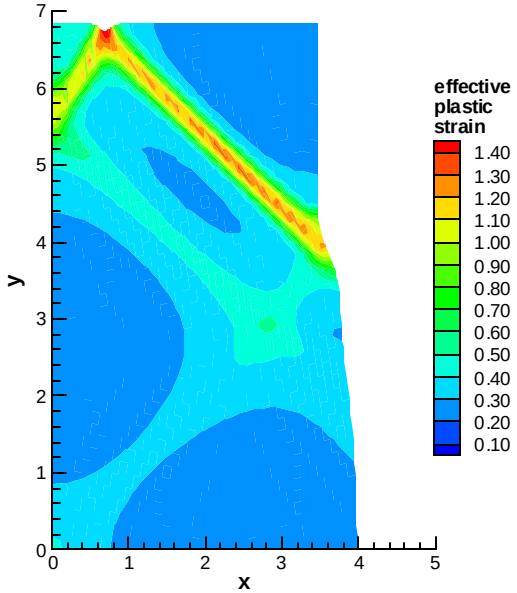


Figure 2. Contours of effective plastic strain for type-II W/NiFe FGM with c = 0.3 at an axial strain of 0.3725.